0026-895X/09/7506-1325–1336$20.00
MOLECULAR PHARMACOLOGY
Copyright © 2009 The American Society for Pharmacology and Experimental Therapeutics
Mol Pharmacol 75:1325–1336, 2009

Vol. 75, No. 6
53470/3475461
Printed in U.S.A.

Elucidation of Binding Sites of Dual Antagonists in the Human Chemokine Receptors CCR2 and CCR5[S]

Spencer E. Hall, Allen Mao, Vicky Nicolaidou, Mattea Finelli, Emma L. Wise, Belinda Nedjai, Julie Kanjanapangka, Paymann Harirchian, Deborah Chen, Victor Selchau, Sofia Ribeiro, Sabine Schyler, James E. Pease, Richard Horuk, and Nagarajan Vaidehi

Department of Immunology, Beckman Research Institute of the City of Hope, Duarte, California (S.E.H., A.M., J.K., N.V.); Leukocyte Biology Section, National Heart and Lung Institute, Imperial College London, London, United Kingdom (V.N., M.F., E.L.W., B.N., J.E.P.); and Berlex Biosciences, Richmond, California (P.H., D.C., V.S., S.R., S.S., R.H.)

Received November 14, 2008; accepted February 27, 2009

ABSTRACT

Design of dual antagonists for the chemokine receptors CCR2 and CCR5 will be greatly facilitated by knowledge of the structural differences of their binding sites. Thus, we computationally predicted the binding site of the dual CCR2/CCR5 antagonist *N*-dimethyl-*N*-[4-[[[2-(4-methylphenyl)-6,7-dihydro-5*H*-benzohepten-8-yl] carbonyl]amino]benzyl]tetrahydro-2*H*-pyran-4-aminium (TAK-779), and a CCR2-specific antagonist *N*-(carbamoylmethyl)-3-trifluoromethyl benzamido-parachlorobenzyl 3-aminopyrrolidine (Teijin compound 1) in an ensemble of predicted structures of human CCR2 and CCR5. Based on our predictions of the protein-ligand interactions, we examined the activity of the antagonists for cells expressing thirteen mutants of CCR2 and five mutants of CCR5. The results show that residues Trp98$^{2.60}$ and Thr292$^{7.40}$ contribute significantly to the efficacy of both TAK-779 and Teijin compound 1, whereas His121$^{3.33}$ and Ile263$^{6.55}$ contribute significantly only to the antagonistic effect of Teijin compound 1 at CCR2. Mutation of residues Trp86$^{2.60}$ and Tyr108$^{3.32}$ adversely affected the efficacy of TAK-779 in antagonizing CCR5-mediated chemotaxis. Y49A$^{1.39}$ and E291A$^{7.39}$ mutants of CCR2 showed a complete loss of CCL2 binding and chemotaxis, despite robust cell surface expression, suggesting that these residues are critical in maintaining the correct receptor architecture. Modeling studies support the hypothesis that the residues Tyr49$^{1.39}$, Trp98$^{2.60}$, Tyr120$^{3.32}$, and Glu291$^{7.39}$ of CCR2 form a tight network of aromatic cluster and polar contacts between transmembrane helices 1, 2, 3, and 7.

The chemokine receptors CCR2 and CCR5 are G protein-coupled receptors (GPCRs) and share approximately 73% sequence identity, mainly in their transmembrane (TM) helices (Charo et al., 1994; Samson et al., 1996). CCR2 is mainly expressed in monocytes, immature dendritic cells, activated T lymphocytes, and basophils and binds several chemokines: CCL2, CCL7, CCL8, and CCL13 (Murphy, 1994). CCR5 is expressed by both $CD4^+$ and $CD8^+$ activated T lymphocytes and monocytes and has three high-affinity ligands, CCL3, CCL4, and CCL5 (Doms and Peiper, 1997). Both CCR2 and CCR5 and their ligands have been implicated in the pathophysiology of a number of diseases, including rheumatoid arthritis and multiple sclerosis (Charo and Ransohoff, 2006; Szekanecz et al., 2006).

Based on their roles in disease, chemokine receptors have been attractive targets for the pharmaceutical industry. Unfortunately, despite a massive effort and numerous clinical trials, only one registered drug, the CCR5 antagonist maraviroc (Selzentry), has thus far resulted from this approach (Lieberman-Blum et al., 2008). The lack of success of chemokine receptor antagonists in the clinic may be due in part to receptor redundancy, and this could explain why these small-molecule antagonists, specific for a single receptor, did not provide a therapeutic effect (Ribeiro and Horuk, 2005). It has been suggested that promiscuous compounds that target more than one receptor might be therapeutically more effective for treating these complex multifactorial diseases (Frantz, 2005; Morphy and Rankovic, 2005).

Knowledge of the structural basis of chemokine receptor

This work was supported by Berlex BioSciences [Grant RCON5924] and by an award from the Arthritis Research Campaign [Grant 18303].

S.E.H. and A.M. contributed equally to this work.

Article, publication date, and citation information can be found at http://molpharm.aspetjournals.org.
doi:10.1124/mol.108.053470.

[S] The online version of this article (available at http://molpharm.aspetjournals.org) contains supplemental material.

ABBREVIATIONS: GPCR, G protein-coupled receptor; TM, transmembrane; TAK-779, *N*,*N*-dimethyl-*N*-[4-[[[2-(4-methylphenyl)-6,7-dihydro-5*H*-benzohepten-8-yl] carbonyl]amino]benzyl]tetrahydro-2*H*-pyran-4-aminium; Teijin compound 1, *N*-(carbamoylmethyl)-3-trifluoromethyl benzamido-parachlorobenzyl 3-aminopyrrolidine; ECL, extracellular loop; HA, hemagglutinin.

subtype selectivity and the receptor conformations stabilized by dual antagonists could help facilitate the design of novel chemokine receptor antagonists. For this reason, we have modeled an ensemble of low-energy, three-dimensional receptor conformations of human CCR2 and CCR5 receptors using the MembStruk4.0 computational method (Hall, 2005; Heo et al., 2007) and predicted the binding sites of a CCR2/CCR5 dual antagonist, TAK-779 (Baba et al., 1999), and a CCR2-specific compound *N*-(carbamoylmethyl)-3-trifluoromethyl benzamido-parachlorobenzyl 3-aminopyrrolidine from Teijin (described as Teijin compound 1) (Moree et al., 2008). The residues in the predicted antagonist binding sites of each receptor were subsequently validated using site-directed mutagenesis and after transient expression, chemotaxis measurements, and radiolabeled chemokine competitive binding experiments were carried out.

Using the class A GPCR numbering system proposed by Ballesteros and Weinstein (1995), we found that the conserved residue Trp98$^{2.60}$ (Trp86$^{2.60}$ in CCR5) contributes significantly to the antagonistic efficacy of TAK-779 in both CCR2 and CCR5, whereas the effect of His121$^{3.33}$ on TAK-779 in CCR2 is replaced by Tyr108$^{3.32}$ in CCR5. The rotational orientation of TM3 is different in CCR2 and CCR5 models, thus positioning these important conserved aromatic residues differently. Comparing the binding sites of TAK-779 and Teijin compound 1 in CCR2, we found that the residues Ile263$^{6.55}$ and Thr292$^{7.40}$ in CCR2 contribute significantly to binding of Teijin compound 1 in CCR2 but not to TAK-779. Residue Glu291$^{7.39}$ in TM7, a highly conserved residue in many CC chemokine receptors, contributes substantially to binding of the protonated Teijin compound 1, and CCL2 but not to the quaternary amine antagonist TAK-779. His121$^{3.33}$ on TM3 and Ile263$^{6.55}$ on TM6 also strongly interact with Teijin compound 1 but only weakly with TAK-779. These differences in the binding of a quaternary and tertiary amine antagonist were predicted by our structural models of CCR2 and subsequently verified by point mutation studies.

We conclude from this study that Glu291$^{7.39}$ can position TM7 in different orientations, thereby generating different receptor conformations. Based on the data from these studies, we postulate that the interhelical contacts Glu291$^{7.39}$, Tyr49$^{1.39}$, Trp98$^{2.60}$, and Tyr120$^{3.32}$ in CCR2 form a receptor activation network. This interaction network between TMs 1, 2, 3, and 7 is formed when Glu291$^{7.39}$ faces TM1 and TM2. We observe that this network is present in our models of the CCR5, CCR3, and CCR1 receptors as well. We hypothesize that this network is required for activation by the chemokine. From our studies, we conclude that an alternative conformation (in which Glu291$^{7.39}$ is facing TM3 and TM6) is stabilized by antagonist binding. Thus the variation in the position of Glu$^{7.39}$ leads to the multiple receptor conformations observed in both CCR2 and CCR5.

Materials and Methods

Materials. Recombinant human CCL2 and CCL3 were from Peprotech EC (London, UK). ^{125}I-Labeled CCL2 and CCL3 were obtained from PerkinElmer Life and Analytical Sciences (Waltham, MA). The monoclonal anti-HA antibody was purchased from Cambridge Bioscience (Cambridge, UK). Fluorescein isothiocyanate-conjugated goat anti-mouse antibody was purchased from Dako UK Ltd. (Ely, UK). All other reagents were purchased from Sigma-Aldrich (Poole, UK) and Invitrogen (Paisley, UK), unless stated otherwise. The CCR2-specific antagonist (Teijin compound 1) shown in Fig. 1 was synthesized as described previously (Moree et al., 2008). TAK-779 [repository number ARP968] was obtained from the Programme European Vaccine against AIDS for AIDS Reagents (National Institute for Biological Standards and Control, UK), supported by the EC FP6/7 Europrise Network of Excellence, AIDS Vaccine I Project and Next Generation HIV-1 Immunogens consortia, and the Bill and Melinda Gates Global HIV Vaccine Research Cryorepository-Collaboration for AIDS Vaccine Discovery Project and was donated by the United States National Institute of Allergy and Infectious Diseases Extramural Activities, distributed with the permission of Takeda Chemical Industries, Ltd (Osaka, Japan).

Molecular Modeling Using the MembStruk4.0. The MembStruk4.0 procedure used in this work has been described in detail previously (Hall, 2005; Heo et al., 2007). Here we describe briefly the methods as applied to CCR2 and CCR5.

The seven TM regions and the hydrophobic maxima for each helix in human CCR2 and CCR5 were predicted using the TM2ndS method (Trabanino et al., 2004). The TM2ndS uses a multiple sequence alignment that includes all human, rat, and mouse chemokine receptor CCR and some CXCR sequences; it predicts the TM region based on the seven maxima in hydrophobicity over the entire sequence alignment. The predicted seven TM regions for both CCR2 and CCR5 are shown in Supplemental Scheme 1.

The next step was to optimize the rotation, translation, and the helical kinks starting from an assembled bundle of the canonical helices built from the TM predictions. Canonical right-handed α-helices were built for each helix, and their helical axes were oriented in space according to the 7.5-Å low-resolution electron density map of frog rhodopsin (Schertler, 1998). This 7.5-Å electron density map gives the positions and the rough relative orientations of the helical axes that serves as the starting point for optimization of the helical bundle. It should be emphasized here that no information was used from any of the crystal structures of GPCRs. The relative translational orientation of the seven helices was optimized by aligning the hydrophobic maximum determined for each helix to a plane. The rotational orientation was optimized using a combination of hydrophobic moments and molecular dynamics techniques. More details of the procedure are given in the Supplemental material. Thus, using the MembStruk4.0 procedure, we derived an ensemble of low-energy TM barrel conformations for both CCR2 and CCR5. The receptor conformations were chosen by maximum number of interhelical hydrogen bonds, and the best total energy of the protein conformation in explicit lipid bilayer. The two low-energy conformations chosen for CCR2 differ in the rotational orientations of TM7, which leads to different orientations of the conserved residues Glu291$^{7.39}$ and Thr292$^{7.40}$. In CCR5, two energetically favorable rotational orientations were found for TM6 and TM7, giving rise to four possible receptor conformations. We selected the receptor conformation with the best score with respect to the number of interhelical hydrogen

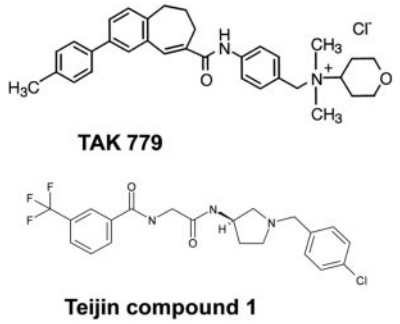

Fig. 1. Chemical structures of the CCR2 and CCR5 dual antagonist TAK-779 and the CCR2-specific antagonist Teijin compound 1. The reported IC_{50} for TAK-779 binding to CCR5 is 1 nM and to CCR2 is 27 nM (Baba et al., 1999). The reported binding affinity of the Teijin compound 1 to CCR2 is 180 nM (Moree et al., 2008).

bonds and the total potential energy of the receptor in explicit lipid bilayer. Extra- and intracellular loops were added using *Whatif* (Vriend, 1990) and the second extracellular loop (ECL) was added using the ECL2 loop of bovine rhodopsin (Protein Data Bank code 1hzx).

Prediction of the Binding Site for the Antagonists TAK-779 and Teijin Compound 1. The antagonists modeled in this study are shown in Fig. 1. We built the ligands using the LigPrep module in the Glide suite from Schrödinger Inc. (New York, NY). Multiple ligand conformations were generated for each of the two ligands using the Monte Carlo method embedded in MacroModel (Schrödinger Inc.). The ligand conformations were clustered using a 1.0-Å root-mean-square deviation cutoff in coordinates, and the lowest energy conformation from each cluster was selected for docking. Each conformation of the ligands was docked using *Glide SP* (Schrodinger Inc.); the top scoring 10 docked conformations were saved and filtered using a cutoff of 80% in ligand buried surface area. The conformations were further refined using MacroModel's Redundant Conformer Elimination, varying the root-mean-square deviation between conformations to reduce the number of clusters of conformations. Next, we performed a complete conjugate gradient minimization of the protein and ligand to 0.1 kcal/mol/Å root mean square in force/atom. We then selected all residues within 5.0 Å of the ligand and optimized them using the side-chain optimizer in Prime (Schrödinger Inc.). The conformations were scored by the binding energies calculated as BE = PE (ligand in fixed protein) − PE (ligand in solvation), where BE is the binding energy, PE (ligand in fixed protein) is the potential energy of the ligand calculated with the protein atoms fixed, and PE (ligand in solvation) is the potential energy of the ligand calculated with the Surface Generalized Born continuum solvation method (Ghosh et al., 1998). The best scoring docked conformation(s) were then visually inspected. Finally, we calculated the contribution of each residue within 5.0 Å of the ligand to the interaction energy of ligand with the receptor.

Generation of Receptor Mutants and Their Transient Expression in L1.2 Cells. pcDNA3.1 plasmids containing human CCR2 and human CCR5 with a 6×HA epitope tag at the N terminus were purchased from the Missouri S&T cDNA Resource Center (http://www.cdna.org). These were subsequently used as a template for the generation of point mutants by polymerase chain reaction using the QuikChange II site-directed mutagenesis kit (Stratagene, Amsterdam, Netherlands) and appropriate oligonucleotide primers. All mutants were verified by DNA sequencing (MWG Biotech, Ebersberg, Germany) before use. The murine pre-B lymphoid cell line L1.2 cells was maintained as described previously (de Mendonça et al., 2005; Vaidehi et al., 2006) in suspension at 37°C with 5% CO_2 at a density of no more than 1×10^6 cells/ml. Plasmids were introduced into L1.2 cells by electroporation as described previously (Vaidehi et al., 2006), which allows for transient, high-level expression of chemokine receptors in a relevant leukocyte background after overnight incubation with 10 mM sodium butyrate.

Flow Cytometry. Transient transfectants were assessed for cell surface expression by flow cytometry after staining with an anti-HA antibody and fluorescein isothiocyanate-conjugated secondary antibody as described previously (Vaidehi et al., 2006).

Chemotaxis Assay. ChemoTx plates (Neuroprobe, Gaithersburg, MD) were used as described previously (Vaidehi et al., 2006) with chemokine placed into the bottom wells in a final volume of 31 μl of chemotaxis media (HEPES-modified RPMI 1640 media containing 0.1% bovine serum albumin). A 5-μm pore filter was placed on top of the wells, and 2×10^5 cells in a volume of 20 μl of chemotaxis media were loaded onto the filter. After incubation for 5 h in a humidified chamber at 37°C with 5% CO_2, cells were scraped from the upper surface of the filter, the filter was removed, and the migrating cells were spun into a white opaque plate using a 96-well funnel plate (Neuroprobe). Cells were counted as described previously (Stroke et al., 2006) by the addition of 30 μl of CellTiter Glo dye (Promega, Southampton, UK) and luminescence measured using a TopCount scintillation counter (PerkinElmer Life and Analytical Sciences). In some assays, a fixed concentration of chemokine was employed in the lower well in the presence or absence of different concentrations of the small molecule antagonists TAK-779 and Teijin compound 1. Migration was reported as the chemotactic index, defined as the ratio of chemokine-driven cell migration to migration to buffer alone. In every experiment, cells transiently expressing WT constructs were employed as a positive control.

Radiolabeled Chemokine Binding Studies. Whole-cell binding assays on transiently transfected L1.2 cells were performed as described previously (de Mendonça et al., 2005; Vaidehi et al., 2006) using 0.1 nM radiolabeled ligand and increasing concentrations of unlabeled homologous chemokine or antagonist. The parameters we used for the binding assays fit the conditions recommended by Daugherty et al. (2000). In brief, all dilutions were carried out in binding buffer (0.1% BSA and 0.05% NaN_3 in RPMI). Previously transfected L1.2 cells were resuspended at 0.5×10^6 cells/25 μl in binding buffer and 25 μl of cells were incubated with 5 μl of 1 nM ^{125}I-CCL2 (CCR2 transfectants) or 5 μl of 1 nM ^{125}I-CCL3 (CCR5 transfectants) together with 20 μl of varying concentrations of unlabeled competing chemokine or antagonist. Binding was allowed to proceed at room temperature for 60 min, after which 50 μl of salt wash (0.4 g in NaCl in 10 ml of binding buffer) was added to each well. The samples were then mixed and layered onto 100 μl of Nyosil oil in a spate tube, and cells were pelleted through the oil by centrifugation at 8500 rpm, for 3 min. Cell-associated radioactivity was counted in a Canberra Packard Cobra 5010 gamma counter (Canberra Packard, Pangebourne, UK). Curve fitting and subsequent data analysis was carried out using the program PRISM and IC_{50} values were obtained by nonlinear regression analysis (GraphPad Software, Inc., San Diego, CA). In all experiments, each data point was assayed in duplicate. Data are presented as the percentage of counts obtained in the absence of unlabeled competing ligand.

Results

Comparison of the Interhelical Contacts of the Predicted Structures of CCR2 and CCR5. Figure 2A shows that in the apoprotein structural model of CCR2. there is a hydrogen bond between Asp88$^{2.50}$ and Asn60$^{1.50}$, and a long (possibly water-mediated) hydrogen bond (8.0 Å) with Asn301$^{7.49}$. This network of hydrogen bonds is highly conserved across class A GPCRs and has been observed in both the rhodopsin and the β2 adrenergic receptor crystal structures (Palczewski et al., 2000; Cherezov et al., 2007). The CCR5 apo-protein structural model also forms a hydrogen bond between Asn48$^{1.50}$ and Asp76$^{2.50}$ and between Asp76$^{2.50}$ and Asn293$^{7.49}$, albeit with increased heavy atom distances between H-bond partners compared with those in CCR2 (Fig. 2B). In addition, we observe a rhodopsin-like interhelical hydrogen bond between Trp165$^{4.50}$ (Trp153$^{4.50}$ in CCR5) and Asn83$^{2.45}$ (Asn71$^{2.45}$ in CCR5), as shown in Fig. 2, A and B.

Our predicted structural models for CCR2 and CCR5 reveal that the TXP motif on TM2, which is conserved in many chemokine receptors including CCR2 and CCR5 (Govaerts et al., 2003), results in a proline kink that points toward TM3 (shown in Supplemental Fig. S2). This kink angle is modulated over a range of 15° to 47° in CCR2 and 17° to 40° in CCR5, as seen from the molecular dynamics simulation of these helices. In contrast, in the rhodopsin sequence the TXP motif is replaced by a GGF motif that places TM2 toward TM7 (Palczewski et al., 2000), similar to the β2 adrenergic receptor (Cherezov et al., 2007).

Trp256$^{6.48}$ (Trp248$^{6.48}$ in CCR5), a highly conserved resi-

due in class A GPCRs, forms an intrahelical hydrogen bond with Asn260$^{6.52}$ (Asn252$^{6.52}$ in CCR5) on TM6. Tyr120$^{3.32}$ (Tyr108$^{3.32}$ in CCR5) and Tyr124$^{3.36}$ (Phe112$^{3.36}$ in CCR5) on TM3 aid in stabilizing the receptors through aromatic ring stacking. There is also an interhelical aromatic ring stacking between Trp256$^{6.48}$ (Trp248$^{6.48}$ in CCR5) and Tyr120$^{3.32}$ (Tyr108$^{3.32}$ in CCR5). We found that the aromatic rings of Trp98$^{2.60}$ and Tyr49$^{1.39}$ do not stack in CCR2, whereas they do in the CCR5 structural model. The position of Glu291$^{7.39}$ is variable in the ensemble of structures. There are two positions for Glu291$^{7.39}$ in CCR2, one in which Glu291$^{7.39}$ is directed toward TM1 and TM2, whereas in the other conformation, Glu291$^{7.39}$ is facing TM3. Depending on which of these conformations is preferred for Glu291$^{7.39}$, the position of Asn301$^{7.49}$ on TM7 makes or breaks an interhelical hydrogen bond with TM2. Likewise, there are two possible orientations of TM7 in CCR5. In the first orientation, Glu283$^{7.39}$ forms interhelical hydrogen bonds with Tyr37$^{1.39}$ and Tyr108$^{3.32}$. In this orientation of TM7, Asn293$^{7.49}$ faces TM6 and possibly forms a water-mediated interhelical hydrogen bond with Asp76$^{2.50}$ on TM2, as described above. The second orientation of TM7 in CCR5 places Glu283$^{7.39}$ toward TM3, retaining the interhelical hydrogen bond with Tyr108$^{3.32}$ and breaking the hydrogen bond with Tyr37$^{1.39}$. Tyr37$^{1.39}$ and Trp86$^{2.60}$ stabilize interhelical interactions with a tight interhelical aromatic stacking interaction.

Predicted Binding site of Teijin Compound 1 and TAK 779 in CCR2. The predicted binding site of Teijin compound 1 and TAK-779 in CCR2 are shown in Fig. 3, A and B. The binding site of the CCR2-specific Teijin compound 1 is located between TM1, TM2, TM3, TM6, and TM7. Figure 3C shows the residues within 5 Å of Teijin compound 1 in CCR2.

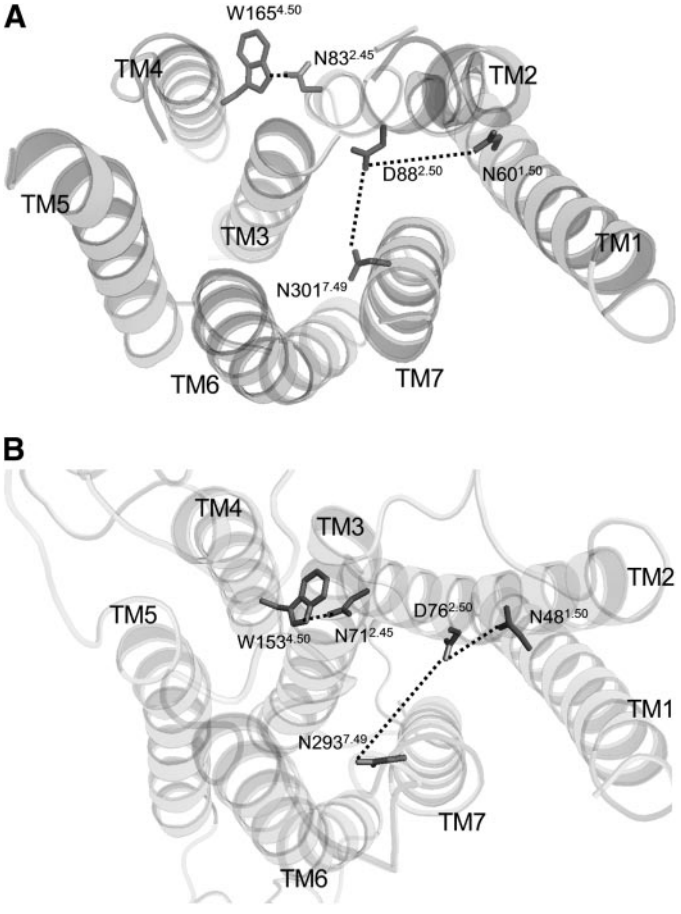

Fig. 2. A, apo-protein structural model of CCR2, one from the ensemble of structural models, showing the hydrogen bond network between Asp88$^{2.50}$ and Asn60$^{1.50}$, and Asn301$^{7.49}$. Another interhelical hydrogen bond is between Trp165$^{4.50}$ and Asn83$^{2.45}$. B, the CCR5 apo-protein structural model showing hydrogen bond network between Asn48$^{1.50}$ and Asp76$^{2.50}$ and Asn293$^{7.49}$. Also the shown is the hydrogen bond between Trp153$^{4.50}$ and Asn71$^{2.45}$. These hydrogen bonds are observed in class A GPCR crystal structures available so far.

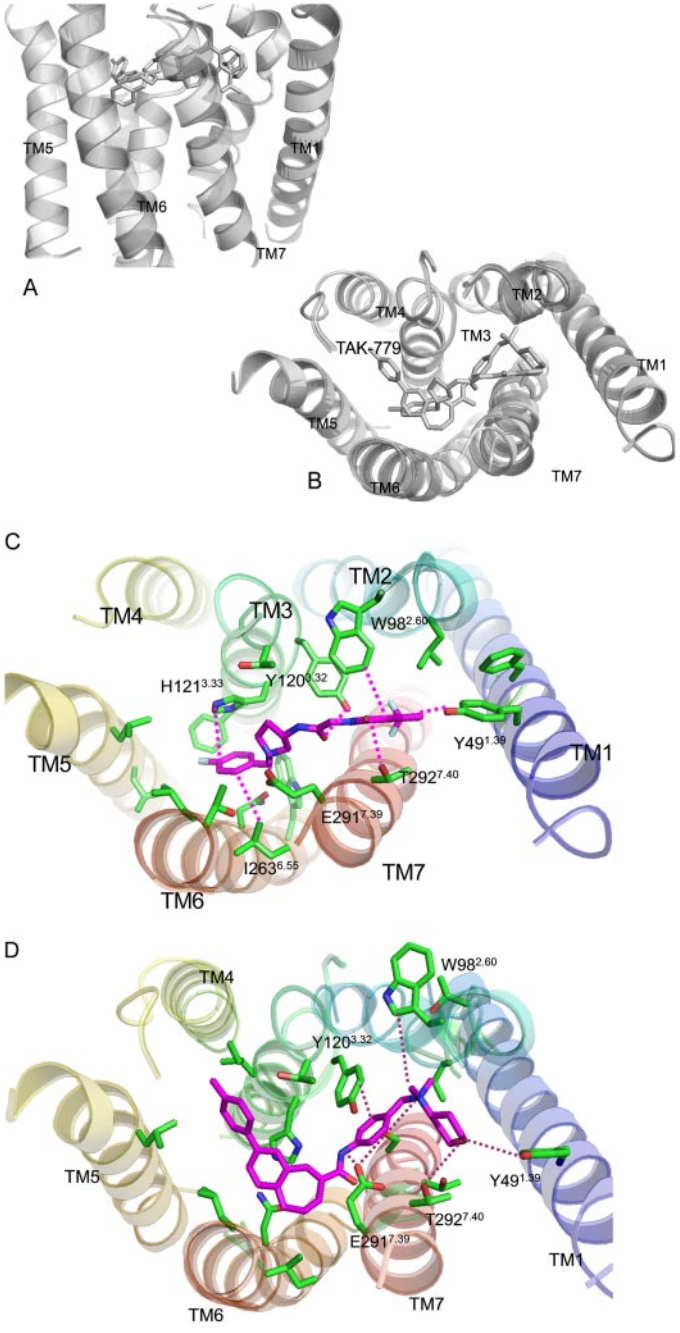

Fig. 3. The predicted structure of human CCR2 with antagonist binding sites. A, side view of the binding site of Teijin compound 1 (green) and TAK-779 (cyan) with the extracellular region at the top (B). Top view of the predicted binding sites of TAK-779 and Teijin compound 1 in the CCR2 binding pocket. C, residues within 5 Å in the binding site of Teijin compound 1. D, residues within 5 Å of the binding site of TAK-779 in CCR2. Dashed lines indicate residues contributing 1 to 5 kcal/mol to the ligand interaction energy.

The strongest protein-ligand interaction, according to our energy calculations, stems from the electrostatic interaction between Glu291$^{7.39}$ and the pyrrolidine nitrogen (distance 2.8 Å). The calculated p*K*a for this group (Jaguar; Schrödinger Inc.) is 7.8 at pH 7.0. Thr292$^{7.40}$ makes a hydrogen bond with the backbone carbonyl group next to the trifluoro phenyl ring. Residues Tyr49$^{1.39}$, Trp98$^{2.60}$, Tyr120$^{3.32}$, His121$^{3.33}$, Trp256$^{6.48}$, Asn260$^{6.52}$, and Ile263$^{6.55}$ contribute approximately 1 to 5 kcal/mol of favorable nonbonded interaction energy, and the dominant contributions among these interactions are van der Waals interaction between the antagonist and Trp98$^{2.60}$, Tyr120$^{3.32}$, and His121$^{3.33}$.

Predicted Binding Site of TAK-779 Antagonist in CCR2. The binding site of TAK-779 in both CCR2 and CCR5 is located between TM1, TM2, TM3, TM6, and TM7, as shown for CCR2 in Fig. 3, A and B. The residues that interact strongly with TAK-779 in CCR2 are shown in Fig. 3D. The strength of the electrostatic interaction of the quaternary amine group of TAK-779 with Glu291$^{7.39}$ is significantly weaker than the interaction with the tertiary amine of Teijin compound 1. The interaction energy of TAK-779 with Thr292$^{7.40}$, Trp98$^{2.60}$, Tyr120$^{3.32}$, and His121$^{3.33}$ are similar to that of Teijin compound 1. In addition, Ile263$^{6.55}$ interacts favorably only with Teijin compound 1 and not with TAK-779. Although the overall interaction energy of Teijin compound 1 with the CCR2 receptor is more favorable, its desolvation penalty lowers its overall predicted binding affinity compared with TAK-779. We predict that the aromatic cluster of Tyr49$^{1.39}$, Trp98$^{2.60}$, Tyr120$^{3.32}$, His121$^{3.33}$, Tyr124$^{3.36}$, and Trp256$^{6.48}$ is a major contributor to the interaction between CCR2 and TAK779.

Experimental Validation of Predicted Binding Sites of Teijin Compound 1 and TAK-779 in CCR2: Surface Expression of Mutant CCR2. To verify the predicted binding sites for TAK-779 and Teijin compound 1, we constructed a series of mutants based on our predictions. These mutants include key residues predicted to be in the binding pocket, such as: Y49A$^{1.39}$, W98A$^{2.60}$, F116A$^{3.28}$, Y120A$^{3.32}$, H121A$^{3.33}$, Y124A$^{3.36}$, F125A$^{3.37}$, W256A$^{6.48}$, I263A$^{6.55}$, E291A$^{7.39}$, E291Q$^{7.39}$, and T292V$^{7.40}$. Cells transfected with the WT receptor or with mutants such as I208A$^{5.44}$, which is not in the predicted binding site for either compound, served as controls. The point mutants, except for F116A$^{3.28}$, Y124A$^{3.36}$, and W256A$^{6.48}$, were all transiently expressed at high levels on the surface of L1.2 cells as detected by flow cytometry after incubation with an antibody to an epitope tag at the receptor amino terminus (Fig. 4A). In the CCR2 model, the residues Tyr124$^{3.36}$ and Trp256$^{6.48}$ form interhelical aromatic interactions that confer stability to the receptor conformation. Mutation of one of these residues has the potential to break this interhelical contact and render the protein misfolded. Phe116$^{3.28}$ π-stacks with Trp98$^{2.60}$ in TM2 in CCR2; hence, its mutation to alanine may destabilize the receptor, resulting in a lack of expression. Previous CCR2 structure-function studies did not include mutations of Phe116$^{3.28}$, Tyr124$^{3.36}$, or Trp256$^{6.48}$ (Mirzadegan et al., 2000; Berkhout et al., 2003).

Chemotaxis Experiments of Functional Point Mutants of CCR2. The same transfectants were subsequently used in chemotaxis assays to assess the effects of mutation on CCR2 function (Fig. 4B). The majority of transfectants behaved similarly to those expressing WT CCR2, exhibiting the bell-shaped concentration response curve typical of these assays, with a maximum response to 1 nM CCL2. The Y120A$^{3.32}$ construct mediated detectable responses at 10 and 100 nM CCL2, whereas Y49A$^{1.39}$ was unresponsive across the entire CCL2 concentration range tested. The point-mutant E291A$^{7.39}$ was unresponsive in chemotaxis, despite being expressed at levels significantly greater than those of WT CCR2. The E291Q$^{7.39}$ mutation restored some of the chemotactic response, suggesting that both the charge and size of this amino acid are critical for receptor activation by the ligand. Cells expressing the F116A$^{3.28}$, Y124A$^{3.36}$, and W256A$^{6.48}$ mutants were unresponsive to all concentrations of CCL2 tested, most likely as a consequence of little or no cell surface expression (data not shown). We observe that the mutants I208A$^{5.44}$, I263A$^{6.55}$, and T292V$^{7.40}$ have surface expression levels comparable with those of WT CCR2 but show greater efficacy in chemotaxis assays. This may be a consequence of GPCR activation being catalytic in nature; therefore, small but detectable decreases in cell surface expression levels will have little effect on downstream signaling as manifested in a chemotaxis assay.

Measurements of Chemotaxis Dependence on the Antagonist Concentration in Functional Mutants of CCR2. The ability of TAK-779 and Teijin compound 1 to inhibit CCL2-mediated chemotaxis in functional mutants of CCR2 was tested. As predicted by molecular modeling, Teijin compound 1 had a reduced ability to inhibit CCL2-mediated chemotaxis of transfectants expressing the H121A$^{3.33}$, I263A$^{6.55}$, and T292V$^{7.40}$ point mutants of CCR2, resulting in significantly reduced IC_{50} values (Fig. 4C and Table 1). Teijin compound 1 had a reduced ability to inhibit CCL2-mediated chemotaxis of transfectants expressing mutants W98A$^{2.60}$, and E291Q$^{7.39}$ (Fig. 4E) at higher concentrations of CCL2 (10–100 nM). In contrast, for TAK-779 only, cells expressing the T292V$^{7.40}$ and W98A$^{2.60}$ constructs showed a significantly reduced inhibitory response, with IC_{50} values of 415 and 142 nM, respectively, compared with an IC_{50} value of 6 nM for WT CCR2 transfectants (Fig. 4, D and F, and Table 1).

Displacement of Radiolabeled CCL2 Measurements for TAK-779 and Teijin Compound 1. To consolidate the data, the ability of each mutant to bind radiolabeled CCL2 was also examined. The resulting IC_{50} values from these measurements are shown in Table 2. The ability of the Teijin compound 1 to displace ^{125}I-CCL2 from transfectants expressing the H121A$^{3.33}$, I263A$^{6.55}$, and T292V$^{7.40}$ mutants was significantly reduced, in accordance with the chemotaxis data for these mutants. Likewise, the ability of TAK-779 to displace ^{125}I-CCL2 from cells expressing the T292V$^{7.40}$ mutant was significantly diminished (IC_{50} of 664 nM compared with 49 nM for WT CCR2), in agreement with the chemotaxis data. No specific binding of the ^{125}I-CCL2 to cells expressing the Y49A$^{1.39}$, W98A$^{2.60}$, Y120A$^{3.32}$, and E291Q$^{7.39}$ mutants was observed, suggesting that mutation lowered the affinity of CCL2 for the receptor beyond the limits of detection in this assay.

In the predicted structure, residues His121$^{3.33}$ and Ile263$^{6.55}$ show favorable van der Waals interactions with the 2,4-dimethylphenyl moiety (see Fig. 3C) of Teijin compound 1. Thr292$^{7.40}$ forms a hydrogen bond with the carbonyl attached to the trifluorotoluyl ring. This is in agreement with the significant change in the IC_{50} values obtained with Teijin compound 1 and transfectants expressing H121A$^{3.33}$,

I263A$^{6.55}$, and T292V$^{7.40}$ mutants. The CCR2 residue Glu291$^{7.39}$ shows strong electrostatic interactions with the pyrrolidine nitrogen [calculated p*K*a (Jaguar; Schrödinger Inc.) is 7.8 at 7.0 pH) and this is in agreement with the observed 2-order-of-magnitude reduction in the antagonistic effect of Teijin compound 1 in chemotaxis assays using 10 nM CCL2 to drive chemotaxis of cells expressing the E291Q$^{7.39}$ mutant. Although specific binding of ^{125}I-CCL2 to cells expressing the CCR2 mutant W98A$^{2.60}$ was undetectable (Table 2), the same transfectants showed reduced sensitivity to

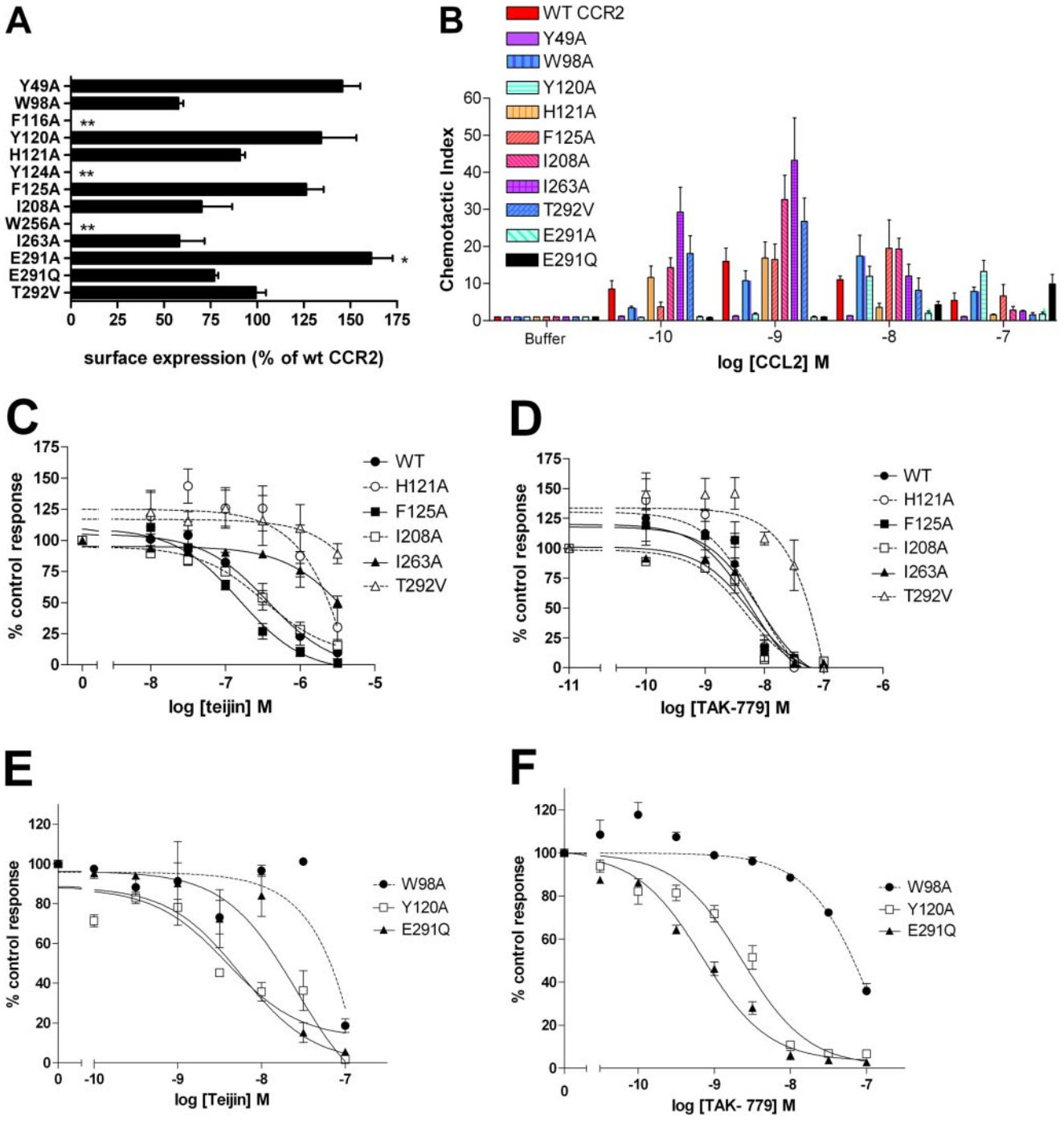

Fig. 4. Receptor expression and inhibition of CCL2-mediated chemotaxis of CCR2 mutants by the antagonists. A, cell surface expression of CCR2 point mutants. Each of the HA-tagged CCR2 point mutant constructs was transiently transfected independently into L1.2 cells as described previously (Vaidehi et al., 2006). Twenty-four hours after transfection, cells were incubated with anti-HA antibody and cell surface expression was analyzed by flow cytometry, after subtraction of irrelevant staining with an isotype control. Surface expression is shown as a percentage of the expression observed for cells simultaneously transfected with the WT CCR2 construct. Data are the mean ± S.E of at least three experiments. B, chemotaxis of CCR2 transfectants to increasing concentrations of CCL2. Data are shown as the chemotactic index and represents the mean ± S.E. from three separate experiments. C and D, chemotaxis of transfectants expressing WT CCR2 or selected CCR2 point mutants to a fixed concentration of 1 nM CCL2 in the presence of increasing concentrations of Teijin compound 1 (C) or TAK-779 (D). The data shown are mean ± S.E. of three separate experiments. E and F, chemotaxis of transfectants expressing WT CCR2 or selected CCR2 point mutants to a fixed concentration of 1 nM CCL2 (WT CCR2), 10 nM CCL2 (W86A and Y120A mutants) and 100 nM CCL2 (E291Q mutant) in the presence of increasing concentrations of Teijin compound 1 (E) or TAK-779 (F). The data shown is the mean mean ± S.E. of three separate experiments.

Teijin compound 1 in chemotaxis assays employing an increased concentration of CCL2 (10 nM). In contrast, the transfectants expressing the F125A$^{3.37}$ and I208A$^{5.44}$ mutants showed no significant change in the IC_{50} values, as we predicted. Likewise, mutation of I208A$^{5.44}$ had little effect on sensitivity to either antagonist, in agreement with our predictions that it lay outside the antagonist binding site.

Iterative Process between Predictions and Experiments. The predicted structure of TAK-779 in CCR2 shows favorable hydrogen bond interactions of Thr292$^{7.40}$ with the oxygen on the tetrahydropyran ring (see Fig. 3D). The predicted binding site is in agreement with experiments with respect to the location of the quaternary amine, tetrahydropyran, and the central phenyl ring. However, contrary to the predictions, H121A$^{3.33}$, F125A$^{3.37}$, and I263A$^{6.55}$ showed no significant changes in the IC_{50} of TAK-779. These data led to the conclusion that we had correctly predicted the binding interactions for the quaternary amine group of TAK-779, the associated tetrahydropyran, and the central phenyl ring but not for the benzocycloheptenyl and the terminal toluyl moieties. Subsequently, we clustered the docked ligand conformations according to their diversity in conformation of the benzocycloheptenyl and toluyl moieties and chose the docked conformation with the best binding energy. In this docking pose, the terminal toulyl ring points away from His121$^{3.33}$, Phe125$^{3.37}$, and Tyr120$^{3.32}$, as indicated by the mutation studies.

Predicted Binding Site of the TAK-779 Antagonist in CCR5. The predicted binding site of TAK-779 in CCR5 is shown in Fig. 5, A and B, and the residues that interact strongly with TAK-779 are shown in Fig. 5C. TAK-779 interacts with TM1, TM2, TM3, TM6, and TM7. Glu283$^{7.39}$ has favorable long range Coulombic interactions with the ligand, in analogy with Glu291$^{7.39}$ in CCR2. It should be noted that this long range Coulombic interaction is not as favorable as the interaction of Glu291$^{7.39}$ with the Teijin compound 1 in CCR2. Residues Trp86$^{2.60}$, Tyr108$^{3.32}$, and Thr284$^{7.40}$ contribute between 2 and 5 kcal/mol to the binding energy. In addition, Leu104$^{3.28}$ and Thr105$^{3.29}$ also show favorable but weaker van der Waals interactions. The distance between Phe109$^{3.33}$ and Phe112$^{3.36}$ and the terminal toluyl ring of TAK-779 is approximately 4.5 Å. Residue Tyr37$^{1.39}$ π-stacks with Trp86$^{2.60}$, which in turn interacts with the quaternary amine group of TAK-779. We found that the contribution of Thr284$^{7.40}$ to the interaction with the TAK-779 is significantly less in CCR5 than in CCR2 (Thr292$^{7.40}$). We picked the top five mutations sorted by their interaction energies with TAK-779: Glu283$^{7.39}$ > Tyr108$^{3.32}$ > Phe109$^{3.33}$ > Tyr37$^{1.39}$ > Trp86$^{2.60}$.

Experimental Validation of the Predicted Binding Site for TAK-779 in CCR5: Surface Expression and Chemotaxis Measurements of Point Mutants of CCR5 to CCL3. A panel of CCR5 point mutants were expressed transiently in L1.2 cells. Figure 6A shows the cell surface

TABLE 1

A summary of data from chemotaxis assays in Fig. 4, C to F, in which the migration of cells expressing WT CCR2 or selected CCR2 point mutants to concentrations of CCL2 (shown in parenthesis next to the mutant name) was inhibited by increasing concentrations of TAK-779 or Teijin compound 1

The data are representative of three experiments. Data are presented as mean ± S.E.

Construct	Antagonist			
	TAK-779		Teijin Compound 1	
	IC_{50}	Log IC_{50}	IC_{50}	Log IC_{50}
	nM	*M*	*nM*	*M*
WT CCR2 (1 nM)	5.78	−8.24 ± 0.20	370.68	−6.43 ± 0.17
W98A$^{2.60}$ (10 nM)	142.23	−6.85 ± 0.33	13,995.87	−4.85 ± 39.64
Y120A$^{3.32}$ (10 nM)	2.29	−8.64 ± 0.08	3.92	−8.41 ± 0.19
H121A$^{3.33}$ (1 nM)	7.42	−8.13 ± 0.21	20,276.82	−4.69 ± 2.70
F125A$^{3.37}$ (1 nM)	7.80	−8.11 ± 0.18	152.26	−6.81 ± 0.11
I208A$^{5.44}$ (1 nM)	4.87	−8.31 ± 0.15	332.66	−6.48 ± 0.10
I263A$^{6.55}$ (1 nM)	6.26	−8.20 ± 0.15	4808.39	−5.32 ± 0.36
E291Q$^{7.39}$ (100 nM)	0.69	−9.16 ± 0.04	26.79	−7.57 ± 0.25
T292V$^{7.40}$ (1 nM)	414.70	−6.38 ± 1.15	N.O.A.	N.O.A.

N.O.A., no observable antagonism (i.e., at ≥1000-fold excess of antagonist, less than 50% inhibition of migration was observed).

TABLE 2

A summary of data from competitive binding experiments

Displacement of ^{125}I-CCL2 from cells expressing WT CCR2 and selected CCR2 point mutants, with increasing concentrations of unlabelled CCL2, TAK-779, or Teijin compound 1. The data are representative of three experiments. Data are presented as mean ± S.E.

Construct	CCL2 Displacement		TAK-779 Displacement		Teijin Compound 1 Displacement	
	IC_{50}	Log IC_{50}	IC_{50}	Log IC_{50}	IC_{50}	Log IC_{50}
	nM	*M*	*nM*	*M*	*nM*	*M*
WT CCR2	9.60	−8.02 ± 0.07	49.30	−7.307 ± 0.39	405.51	−6.392 ± 0.09
Y49A$^{1.39}$	N.S.B.	N.S.B.	N.S.B.	N.S.B.	N.S.B.	N.S.B.
W98A$^{2.60}$	N.S.B.	N.S.B.	N.S.B.	N.S.B.	N.S.B.	N.S.B.
Y120A$^{3.32}$	N.S.B.	N.S.B.	N.S.B.	N.S.B.	N.S.B.	N.S.B.
H121A$^{3.33}$	4.18	−8.38 ± 0.03	19.90	−7.70 ± 0.04	1127.20	−5.948 ± 0.43
I263A$^{6.55}$	3.18	−8.50 ± 0.04	12.85	−7.89 ± 0.03	787.05	−6.104 ± 0.13
E291Q$^{7.39}$	N.S.B.	N.S.B.	N.S.B.	N.S.B.	N.S.B.	N.S.B.
T292V$^{7.40}$	9.18	−8.04 ± 0.12	663.74	−6.178 ± 9.34	N.O.D.	N.O.D.

N.S.B., no specific binding (i.e., at a 1000-fold excess of unlabeled CCL2, less than 50% displacement of ^{125}I-CCL2 was observed). N.O.D., no observable displacement (i.e., at ≥1000-fold excess of antagonist, less than 50% displacement of ^{125}I-CCL2 was observed).

expression of the constructs relative to that of WT CCR5 as deduced by flow cytometry. Unlike CCR2, CCR5 was more tolerant to point mutations; only the W86A$^{2.60}$ and Y108A$^{3.32}$ mutations resulted in modest reductions in cell surface expression. The same transfectants were subsequently used in chemotaxis assays to assess the effects of mutation on receptor function (Fig. 6B). The majority of transfectants behaved similarly to those expressing WT CCR5, exhibiting bell-shaped dose response curves with a maximum response to 30 nM CCL3. It is noteworthy that the cells expressing the Y37A$^{1.39}$ mutant of CCR5 were completely unresponsive to CCL3 across the concentration range of CCL3 examined.

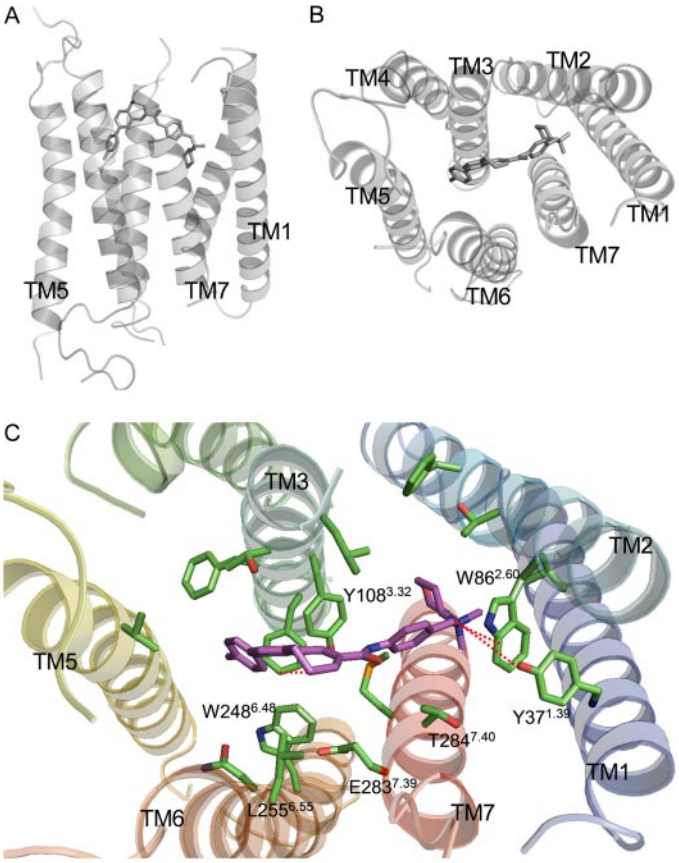

Fig. 5. The predicted structure of human CCR5 with TAK-779 bound. A, side view of the binding site of TAK-779 (shown in pink) in CCR5 with the extracellular region at the top. B, top view of the predicted binding site of TAK-779 in CCR5. C, details of the predicted binding site showing all residues within 5 Å for TAK-779 in CCR5.

Modeling suggests that Tyr37$^{1.39}$ in TM1 π-stacks with Trp86$^{2.60}$ on TM2, and therefore the Y37A$^{1.39}$ mutation may lead to a receptor conformation that prevents CCL3 binding and activation. The importance of the aromatic residues in CCR5 was also highlighted by a previous study (Govaerts et al., 2003), which suggested that several aromatic residues within TM2, -3, and -6 formed important intra- and inter-helical contacts responsible for maintaining an active receptor conformation. In contrast, cells expressing the F109A$^{3.33}$ construct were responsive to CCL3 and exhibited a left-shifted dose-response curve compared with cells expressing WT CCR5, suggesting that the mutant receptor had higher affinity for CCL3 than the WT receptor (Table 3). This was confirmed by homologous competition binding assays in which ^{125}I-CCL3 was displaced by unlabeled CCL3 from cells expressing either WT or mutant CCR5 (Table 4).

Measurements on Concentration Dependence of Antagonism in Functional Mutants of CCR5. Functional mutants were then assessed for their ability to be antagonized by TAK-779 in chemotaxis assays using a fixed concentration of 30 nM CCL3 (Fig. 6C). As predicted by modeling, cells expressing the W86A$^{2.60}$ and Y108A$^{3.32}$ mutants showed a large rightward shift in the concentration-response curve, indicative of a significantly reduced sensitivity to antagonism by TAK-779. In contrast, the F109A$^{3.33}$ and E283Q$^{7.39}$ mutations had little effect on the potency of TAK-779 compared with WT CCR5, with a modest increase in IC_{50} values (Table 4). Notable were the findings that the W86A$^{2.60}$ and Y108A$^{3.32}$ constructs exhibited a loss in TAK-779 activity of greater than 2 orders of magnitude. The ability of

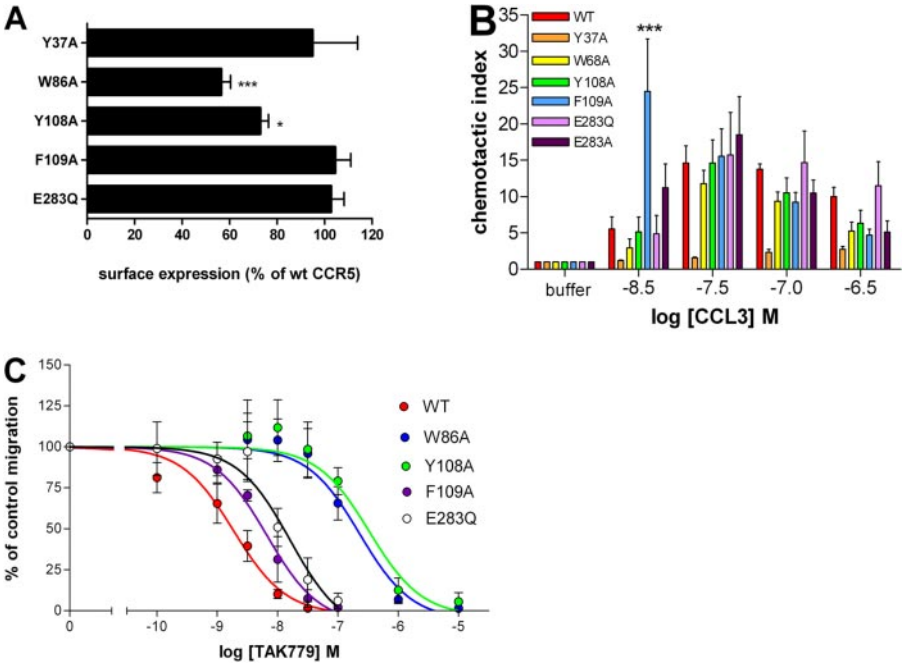

Fig. 6. Receptor expression and CCL3-mediated chemotaxis of CCR5 mutants. A, cell-surface expression of CCR5 mutants relative to that of WT CCR5. Data represent the mean ± S.E. from eight separate experiments. ***, $p < 0.001$; *, $p < 0.05$, compared with WT CCR5 expression as deduced by two-way analysis of variance and Bonferroni's multiple comparisons test. B, chemotaxis of CCR5 transfectants to increasing concentrations of CCL3. Data are shown as the chemotactic index and represents the mean ±S.E. from three separate experiments. ***, $p < 0.001$ compared with WT CCR5 transfectants as deduced by two-way analysis of variance and Bonferroni's multiple comparisons test. C, chemotaxis of transfectants expressing WT CCR5 or selected CCR5 point mutants to a fixed concentration of 30 nM CCL3 in the presence of increasing concentrations of TAK-779. The data shown is the mean of three to five separate experiments ± S.E.

TAK-779 to displace ^{125}I-CCL3 from each mutant was also examined. In ^{125}I-CCL3 binding studies, cells expressing the W86A$^{2.60}$, Y108A$^{3.32}$, F109A$^{3.33}$, and E283Q$^{7.39}$ constructs exhibited reduced sensitivity to TAK-779 compared with WT CCR5, W86A$^{2.60}$ and Y108A$^{3.32}$ transfectants showing the greatest loss of sensitivity to the antagonist (Table 4). This is supportive of the chemotaxis data.

In contrast to Teijin compound 1, we predicted that Glu291$^{7.39}$ would have little effect on the IC_{50} of TAK-779 in both CCR2 and CCR5, because the quaternary amines of the compound can interact favorably with aromatic residues through cation-π interactions (Gallivan and Dougherty, 1999), rather than forming a salt bridge. This is in complete agreement with our data, where the E283Q$^{7.39}$ mutant (which retains the polar nature of the glutamate residue) does not significantly affect TAK-779 antagonist activity. In the predicted binding model of TAK-779 in CCR5 (Fig. 5C), Trp86$^{2.60}$ has favorable cation-π interactions with the quaternary amine group on TAK-779, and indeed mutation of Trp86$^{2.60}$ resulted in the largest change in IC_{50}. Residue Tyr108$^{3.32}$ shows favorable van der Waals interactions with both the central phenyl and cycloheptenyl ring of TAK-779, and mutation of this residue significantly lowers its IC_{50} value 70-fold.

Discussion

Lack of Chemotaxis by Some CCR2 and CCR5 Mutants. Cells expressing the CCR2 point mutants Y49A$^{1.39}$, and E291A$^{7.39}$ showed no detectable CCL2 binding and no chemotactic responses to CCL2, whereas the mutants W98A$^{2.60}$, Y120A$^{3.32}$, and E291Q$^{7.39}$ showed chemotactic responses only at relatively high concentrations of CCL2 (10–100 nM) and no specific binding of 0.1 nM ^{125}I-CCL2 (Tables 1 and 2). In contrast, the corresponding mutants in CCR5, except for Y37A$^{1.39}$, showed binding and chemotactic response to CCL3. It is noteworthy that the Y37A$^{1.39}$ mutant of CCR5 does show activity in HIV viral entry studies (Dragic et al., 2000; Seibert et al., 2006). How can we account for the lack of response of these CCR2 mutants, given their expression at levels comparable with those of the wild-type receptors? Studies have shown that residues in the amino terminus of several chemokines are required for inducing signaling through their respective receptors (Allen et al., 2007). For example, truncation of the amino terminus of CCL2 converts it into a high-affinity antagonist for CCR2 (Gong and Clark-Lewis, 1995; Zhang and Rollins, 1995; Jarnagin et al., 1999). Thus, we hypothesize that the first few residues in the amino terminus of CCL2 interact with residues Tyr49$^{1.39}$, Trp98$^{2.60}$, Tyr120$^{3.32}$, and Glu291$^{7.39}$ in CCR2 in the active receptor state. Residues Tyr49$^{1.39}$ (Tyr37$^{1.39}$ in CCR5), Trp98$^{2.60}$ (Trp86$^{2.60}$ in CCR5), Tyr120$^{3.32}$ (Tyr108$^{3.32}$ in CCR5), and Glu291$^{7.39}$ (Glu283$^{7.39}$ in CCR5) form a tight interhelical network as observed in the models of both CCR2 and CCR5 (Supplemental Fig. S1, A and B). The amino terminus of CCL2 activates CCR2 by strengthening this interhelical network, because the second residue in CCL2, which is a Lys, could form a strong salt bridge with Glu291$^{7.39}$ in CCR2, and trigger receptor activation. This residue is a Gln in CCL3, and therefore the receptor mutation E283Q$^{7.39}$ in CCR5 does not affect the activation of CCR5 by CCL3. Thus, based on our experimental and modeling data, we postulate that the interhelical contacts observed in the region between Glu291$^{7.39}$, Tyr49$^{1.39}$, Trp98$^{2.60}$, and Tyr120$^{3.32}$ form an essential network stabilizing the receptor in the active state, whereas antagonists such as Teijin and TAK-779 bind to disrupt this network and lock it in an inactive conformation.

Binding Site of TAK-779 in CCR2 and CCR5. Table 5 shows the list of residues we have found to be important in binding of the two antagonists in both CCR2 and CCR5. Comparisons of the effect of mutation upon the binding site of TAK-779 in both CCR2 and CCR5 show that the residues Trp98$^{2.60}$ of CCR2 and Trp86$^{2.60}$ in CCR5 are both used by TAK-779. In contrast, TAK-779 contacts Tyr108$^{3.32}$ of CCR5 but not Tyr120$^{3.32}$ of CCR2. Residues His121$^{3.33}$ (Phe109$^{3.33}$ in CCR5), and Glu291$^{7.39}$ (Glu283$^{7.39}$ in CCR5) are not used by TAK-779 to antagonize either CCR2 or CCR5 but are used by Teijin compound 1 to antagonize CCR2.

TABLE 3

A summary of data from chemotaxis assays in Figures 6C, where the migration of cells expressing WT CCR5 or selected CCR5 point mutants to a fixed concentration of 30 nM CCL3 was inhibited by increasing concentrations of TAK-779

The data are representative of three to five experiments. Data are presented as mean ± S.E.

Construct	TAK-779	
	IC_{50}	Log IC_{50}
	nM	*M*
WT CCR5	1.86	−8.73 ± 0.11
W86A$^{2.60}$	229.09	−6.64 ± 0.20
Y108A$^{3.32}$	331.13	−6.48 ± 0.22
F109A$^{3.33}$	6.61	−8.18 ± 0.11
E283Q$^{7.39}$	16.22	−7.79 ± 0.22

TABLE 4

A summary of data from competitive binding experiments

Displacement of ^{125}I-CCL3 from cells expressing WT CCR5 and selected CCR5 point mutants, with increasing concentrations of unlabelled CCL3 or TAK-779. The data are representative of three or four experiments.

Construct	Competing Ligand			
	CCL3		TAK-779	
	IC_{50}	Log IC_{50}	IC_{50}	Log IC_{50}
	nM	*M*	*nM*	*M*
WT CCR5	28.12	−7.55 ± 0.16	7.12	−8.15 ± 0.10
W86A$^{2.60}$	32.26	−7.51 ± 0.29	N.O.D.	N.O.D.
Y108A$^{3.32}$	29.51	−7.53 ± 0.51	N.O.D.	N.O.D.
F109A$^{3.33}$	12.44	−7.91 ± 0.24	14.45	−7.84 ± 0.19
E283Q$^{7.39}$	52.84	−7.28 ± 0.56	11.59	−7.94 ± 0.16

N.O.D., no observable displacement (i.e., at a 1000-fold excess of unlabeled ligand, less than 50% displacement of ^{125}I-CCL3 was observed).

TAK-779 is a dual antagonist with 1 and 27 nM binding affinity for CCR5 and CCR2, respectively (Baba et al., 1999). Examination of the functional groups of TAK-779 that interact with particular residues shows that the charge of the quaternary amine in TAK-779 is delocalized on the alkyl substituents, leading to predicted preferred interactions with the aromatic residues Tyr49$^{1.39}$, Trp98$^{2.60}$, Tyr120$^{3.32}$ in CCR2 and Tyr37$^{1.39}$, Trp86$^{2.60}$, and Tyr108$^{3.32}$ in CCR5, rather than forming a salt bridge with Glu291$^{7.39}$ (Glu283$^{7.39}$ in CCR5). The benzocycloheptenyl moiety of TAK-779 is buried in the TM regions of CCR2, whereas in CCR5, it points toward ECL2 (Supplemental Fig. S3). The terminal toluyl moiety of TAK-779 has a similar location in both CCR2 and CCR5. Thus, although the overall binding site for TAK-779 is similar in CCR2 and CCR5, the contributions of individual amino acids to antagonist binding vary.

Binding Site of Teijin Compound 1 and TAK-779 in CCR2. The binding site of both TAK-779 and Teijin compound 1 in CCR2 is located between TM1, TM2, TM3, TM6, and TM7. Although the antagonists share a binding region, the energy contribution of certain residues to ligand binding is different. This difference in contribution could be due to side-chain orientation or difference in ligand orientation. Residues Trp98$^{2.60}$ and Thr292$^{7.40}$ contribute differentially to binding of TAK-779 and Teijin compound 1, whereas residues His121$^{3.33}$, Glu291$^{7.39}$, and Ile263$^{6.55}$ contribute only to Teijin compound 1 and have very negligible contributions to TAK-779, as shown in Table 5. In CCR2, Glu291$^{7.39}$ contributes less to TAK-779 than to Teijin compound 1 binding (Berkhout et al., 2003). In addition, the orientation of Glu291$^{7.39}$ differs in the TAK-779- and the Teijin compound 1-bound CCR2 structures. We believe that subtype selectivity of Teijin compound 1 for CCR2 could arise from the differential contributions from residues His121$^{3.33}$, Ile263$^{6.55}$, and Glu291$^{7.39}$. One pitfall that we have observed in the CCR2 model is that Tyr120$^{3.32}$ was predicted to have significant interaction with both Teijin compound 1 and TAK-779 in CCR2. Mutation suggested that this is not the case. We believe that Tyr120$^{3.32}$ may still have an effect on the binding of other antagonists, and the effect of the ligand-induced conformational changes in the receptor upon binding could allow Tyr120$^{3.32}$ to move out of the binding pocket for TAK-779 and Teijin compound 1. Work to study these conformational changes using the computational methods described in Bhattacharya et al. (2008) is under way.

Comparison of the Antagonist Binding Site in CCR2 and CCR5 to Other CCR Chemokine Receptors and Other Class A GPCRs. Although the residues shown to be important for antagonist activity in CCR2 and CCR5 may not be strictly extrapolated to other chemokine receptors and class A GPCRs, we have attempted to put these results in perspective for sake of comparison. Table 6 shows a comparison of relative importance of various residues in the binding pocket of antagonists studied for the four chemokine recep-

TABLE 5

Summary of the mutation results and its effect on inhibition by Teijin compound and TAK-779 in CCR2 and CCR5

The results compiled here are from this study only.

Mutants		Expression Level		Chemotaxis Activity		Teijin Compound 1 in CCR2	TAK-779	
CCR2	CCR5	CCR2	CCR5	CCR2	CCR5		CCR2	CCR5
Y49A$^{1.39}$	Y37A$^{1.39}$	↑	↑	Nil	Nil	Nil	Nil	Nil
W98A$^{2.60}$	W86A$^{2.60}$	↓	↑	↓	WT	↑	↑	↑
F116A$^{3.28}$	N.A.	Nil	N.A.	Nil	N.A.	Nil	Nil	N.A.
Y120A$^{3.32}$	Y108A$^{3.32}$	↑	↑	↓	WT	↓	↓	↑
H121A$^{3.33}$	F109A$^{3.33}$	WT	↑	WT	WT	↑	↓	↓
Y124A$^{3.36}$	N.A.	Nil	N.A.	Nil	N.A.	Nil	Nil	N.A.
F125A$^{3.37}$	N.A.	↑	N.A.	WT	N.A.	N.G.	N.G.	N.A.
I208A$^{5.44}$	N.A.	WT	N.A.	↑	N.A.	N.G.	N.G.	N.A.
W256A$^{6.48}$	N.A.	Nil	N.A.	Nil	N.A.	Nil	Nil	N.A.
I263A$^{6.55}$	N.A.	↓	N.A.	↑	N.A.	↑	↓	N.A.
E291A$^{7.39}$	N.A.	↑	N.A.	Nil	N.A.	N.A.	N.A.	N.A.
E291Q$^{7.39}$	E283Q$^{7.39}$	WT	↑	↓	↓	↑	↓	↓
T292V$^{7.40}$	N.A.	WT	N.A.	↑	N.A.	↑	↑	N.A.

WT, wild type (or same as wild type); ↑, higher than WT; ↓, lower than WT; N.A., not available or performed in this study; N.G., negligible effect; Nil, negligible or nil expression.

TABLE 6

List of conserved residues in four chemokine receptors that have been mutated to alanine in this and other published studies (Dragic et al., 2000; Mirzadegan et al., 2000; Berkhout et al., 2003; de Mendonça et al., 2005; Maeda et al., 2006; Seibert et al., 2006; Wise et al., 2007)

Mutation of the underlined and bold residues has been reported to display a loss of antagonist activity. Residues in parentheses have no significant effect on either agonist or antagonist activity; italic residues indicate mutants with poor cell surface expression and/or reduced chemotactic activity compared with wild-type receptor; residues in normal type and not in parentheses have not been mutated; and underlined and italic residues have significant effect on small molecule agonist activity. Glu7.39 mutation results are for E7.39Q mutation and not the alanine mutation.

CCR1	CCR2	CCR3	CCR5
Tyr41$^{1.39}$	*Tyr49*$^{1.39}$	*Tyr41*$^{1.39}$	**Tyr37$^{1.39}$**
(Trp90$^{2.60}$)	**Trp98$^{2.60}$**	Trp86$^{2.60}$	**Trp86$^{2.60}$**
Tyr113$^{3.32}$	**Tyr120$^{3.32}$**	**Tyr113$^{3.32}$**	**Tyr108$^{3.32}$**
Tyr114$^{3.33}$	**His121$^{3.33}$**	His114$^{3.33}$	(Phe109$^{3.33}$)
Leu117$^{3.36}$	*Tyr124*$^{3.36}$	Leu117$^{3.36}$	Tyr112$^{3.36}$
(Trp252$^{6.48}$)	*Trp256*$^{6.48}$	Trp252$^{6.48}$	Trp248$^{6.48}$
Ile259$^{6.55}$	**Ile263$^{6.55}$**	Ile259$^{6.55}$	(Leu255$^{6.55}$)
Glu287$^{7.39}$	**Glu291$^{7.39}$**	**Glu287$^{7.39}$**	**Glu283$^{7.39}$**
Val288$^{7.40}$	**Thr292$^{7.40}$**	Val288$^{7.40}$	Thr284$^{7.40}$

tors, CCR1, CCR2, CCR3 and CCR5. Tyr1.39, Tyr3.32, and Trp2.60 are conserved across CCR1 to CCR9 chemokine receptors. Tyr1.39 and Tyr3.32 have significant effect on either agonist or antagonist binding in all the four CCR1 (de Mendonça et al., 2005), CCR2 (Berkhout et al., 2003), CCR3 (Wise et al., 2007), and CCR5 (Dragic et al., 2000; Maeda et al., 2006; Seibert et al., 2006) chemokine receptors, and Trp2.60 has significant effect on antagonist inhibition only in CCR2 and CCR5. Based on our models of these four receptors, we observed that Trp2.60 is positioned more in the interhelical region between TM2 and TM3 in CCR1 and CCR3 and inside the binding pocket in CCR5. In the CCR2 model, Trp2.60 is well positioned toward the ligand for Teijin compound 1 binding and not for TAK-779. His3.33 is not strictly conserved in all the four chemokine receptors but has significant effect on antagonist inhibition in CCR1 and CCR2 and not in CCR5 for the inhibition effect of TAK-779. It is noteworthy that comparison of this binding site with the known ZM241385 (antagonist) binding site in human adenosine A2A receptor crystal structure (Jaakola et al., 2008) shows that the residue corresponding to the position 3.33 is Leu85$^{3.33}$ in the human A2A receptor and shows strong van der Waals contact with the aromatic ring system in ZM241385. Positions 3.36 and 6.48 in CCR2 seem to be important for the expression of the receptor and may be related to the interhelical interactions. Position 6.55 is critical in subtype selectivity, because it shows substantial effect on antagonist inhibition in CCR2 for both TAK-779 and Teijin compound 1 and has no effect on TAK-779 in CCR5 for HIV viral entry (Dragic et al., 2000). This position 6.55 is also critical to differentiating two different antagonists for the same receptor. For example, mutation of I259A$^{6.55}$ in CCR1 leads to substantial lowering of inhibition for BX471 (Vaidehi et al., 2006) and not for UCB35625 (de Mendonça et al., 2005). It is noteworthy that the corresponding residue in A2A crystal structure, Asn253$^{6.55}$ makes two hydrogen bonds with the bicyclic triazolotriazine ring system in ZM241385, and this could contribute to the subtype specificity of ZM241385 (Jaakola et al., 2008). Glu7.39 is an important residue for agonist and antagonist activity in all the four chemokine receptors, CCR1, CCR2, CCR3, and CCR5. This position is Ile274$^{7.39}$ in A2A, and makes a weak hydrophobic interaction in the A2A crystal structure. We have compared the binding site of antagonists in the chemokine receptors only to the A2A crystal structure because of the similarities in the nature of the antagonists studied here and ZM241385.

Conclusions

Using a combination of computational predictions followed by site-directed mutagenesis, radiolabeled binding, and chemotaxis experiments, we observe that the structurally distinct Teijin and TAK-779 antagonists bind in slightly different but overlapping intrahelical transmembrane pockets in CCR2. A group of five conserved residues, Trp98$^{2.60}$, His121$^{3.33}$, Ile263$^{6.55}$, Glu291$^{7.39}$, and Thr292$^{7.40}$ play a critical role in the activity of Teijin compound 1 at CCR2, whereas only Trp98$^{2.60}$ and Thr292$^{7.40}$ of this group play an important role in TAK-779 activity. Mutation of Trp86$^{2.60}$ and Tyr108$^{3.32}$ significantly affects the activity of TAK-779 at CCR5. We also observed that mutation of Y49A$^{1.39}$, W98A$^{2.60}$, Y120A$^{3.32}$, and E291Q$^{7.39}$ of CCR2 severely reduced the affinity of the receptor for CCL2. We hypothesize that these residues are involved in a network of interhelical interactions, and disruption of the network leads to reduced binding and potency efficacy of the agonist CCL2. Glu291$^{7.39}$ of CCR2 and Glu283$^{7.39}$ in CCR5 play an important role in mediating receptor conformations stabilized by either antagonist, leading to an ensemble of receptor conformations.

In this work, we have demonstrated an iterative process between computational predictions and experimental validation, where the experimental results were subsequently used to reexamine and refine the docked conformations of TAK-779 in CCR2. The effective process of computationally predicting testable hypotheses has led not only to a reduction of the number of experiments but also to valuable insights into the role of Glu291$^{7.39}$ in mediating the conformational flexibility of the CCR2 and CCR5 receptors. Based on the results, we hypothesize that a receptor activation network located between TMs 1, 2, and 7 and consisting of the highly conserved residues Tyr49$^{1.39}$, Trp98$^{2.60}$, Tyr120$^{3.32}$, and Glu291$^{7.39}$ is either stabilized in an active state by the agonist or disrupted by an antagonist. It should be noted that these residues are not strictly conserved across all the CC chemokine receptors, suggesting that a "one size fits all" model of chemokine receptor activation/antagonism will not be forthcoming.

References

Allen SJ, Crown SE, and Handel TM (2007) Chemokine: receptor, structure, interactions and antagonism. *Annu Rev Immunol* **25:**787–820.

Baba M, Nishimura O, Kanzaki N, Okamoto M, Sawada H, Iizawa Y, Shiraishi M, Aramaki Y, Okonogi K, Ogawa Y, et al. (1999) A small-molecule, nonpeptide CCR5 antagonist with highly potent and selective anti-HIV-1 activity. *Proc Natl Acad Sci U S A* **96:**5698–5703.

Ballesteros J and Weinstein J (1995) Integrated methods for modeling G-protein coupled receptors. *Methods Neurosci* **25:**366–428.

Berkhout TA, Blaney FE, Bridges AM, Cooper DG, Forbes IT, Gribble AD, Groot PH, Hardy A, Ife RJ, Kaur R, et al. (2003) CCR2: characterization of the antagonist binding site from a combined receptor modeling/mutagenesis approach. *J Med Chem* **46:**4070–4086.

Bhattacharya S, Hall SE, and Vaidehi N (2008) Agonist-induced conformational changes in bovine rhodopsin: insight into activation of G-protein-coupled receptors. *J Mol Biol* **382:**539–555.

Charo IF, Myers SJ, Herman A, Franci C, Connolly AJ, and Coughlin SR (1994) Molecular cloning and functional expression of two monocyte chemoattractant protein 1 receptors reveals alternative splicing of the carboxyl-terminal tails. *Proc Natl Acad Sci U S A* **91:**2752–2756.

Charo IF and Ransohoff RM (2006) The many roles of chemokines and chemokine receptors in inflammation. *N Engl J Med* **354:**610–621.

Cherezov V, Rosenbaum DM, Hanson MA, Rasmussen SG, Thian FS, Kobilka TS, Choi HJ, Kuhn P, Weis WI, Kobilka BK, et al. (2007) High-resolution crystal structure of an engineered human beta2-adrenergic G protein-coupled receptor. *Science* **318:**1258–1265.

Daugherty BL, Siciliano SJ, and Springer MS (2000) Radiolabeled chemokine binding assays. *Methods Mol Biol* **138:**129–134.

de Mendonça FL, da Fonseca PC, Phillips RM, Saldanha JW, Williams TJ, and Pease JE (2005) Site-directed mutagenesis of CC chemokine receptor 1 reveals the mechanism of action of UCB 35625, a small molecule chemokine receptor antagonist. *J Biol Chem* **280:**4808–4816.

Doms RW and Peiper SC (1997) Unwelcomed guests with master keys: how HIV uses chemokine receptors for cellular entry. *Virology* **235:**179–190.

Dragic T, Trkola A, Thompson DA, Cormier EG, Kajumo FA, Maxwell E, Lin SW, Ying W, Smith SO, Sakmar TP, et al. (2000) A binding pocket for a small molecule inhibitor of HIV-1 entry within the transmembrane helices of CCR5. *Proc Natl Acad Sci U S A* **97:**5639–5644.

Frantz S (2005) Drug discovery: playing dirty. *Nature* **437:**942–943.

Gallivan JP and Dougherty DA (1999) Cation-pi interactions in structural biology. *Proc Natl Acad Sci U S A* **96:**9459–9464.

Ghosh A, Rapp CS, and Friesner RA (1998) Generalized Born model based on a surface integral formulation. *J Phys Chem B* **102:**10983–10990.

Gong JH and Clark-Lewis I (1995) Antagonists of monocyte chemoattractant protein 1identified by modification of functionally critical NH2-terminal residues. *J Exp Med* **181:**631–640.

Govaerts C, Bondue A, Springael JY, Olivella M, Deupi X, Le Poul E, Wodak SJ, Parmentier M, Pardo L, and Blanpain C (2003) Activation of CCR5 by Chemokines Involves an Aromatic Cluster between Transmembrane Helices 2 and 3. *J Biol Chem* **278:**1892–1903.

Hall SE (2005) Development of structure prediction methods for G-protein coupled receptors, Ph.D. Thesis, California Institute of Technology, Pasadena, CA.

Heo J, Vaidehi N, Wendel J, and Goddard WA 3rd (2007) Prediction of the 3D structure of rat MrgA GPCR and identification of its binding site. *J Mol Graph Model* **26:**800–812.

Jaakola VP, Griffith MT, Hanson MA, Cherezov V, Chien EY, Lane JR, IJzerman AP, and Stevens RC (2008) The 2.6 angstrom crystal structure of a human A2A adenosine receptor bound to an antagonist. *Science* **322:**1211–1217.

Jarnagin K, Grunberger D, Mulkins M, Wong B, Hemmerich S, Paavola C, Bloom A, Bhakta S, Diehl F, Freedman R, et al. (1999) Identification of surface residues of the monocyte chemotactic protein 1 that affect signaling through the receptor CCR2. *Biochemistry* **38:**16167–16177.

Lieberman-Blum SS, Fung HB, and Bandres JC (2008) Maraviroc: a CCR5-receptor antagonist for the treatment of HIV-1 infection. *Clin Ther* **30:**1228–1250.

Maeda K, Das D, Ogata-Aoki H, Nakata H, Miyakawa T, Tojo Y, Norman R, Takaoka Y, Ding J, Arnold GF, et al. (2006) Structural and molecular interactions of CCR5 inhibitors with CCR5. *J Biol Chem* **281:**12688–12698.

Mirzadegan T, Diehl F, Ebi B, Bhakta S, Polsky I, McCarley D, Mulkins M, Weatherhead GS, Lapierre JM, Dankwardt J, et al. (2000) Identification of the binding site for a novel class of CCR2b chemokine receptor antagonists—binding to a common chemokine receptor motif within the helical bundle. *J Biol Chem* **275:** 25562–25571.

Moree WJ, Kataoka K, Ramirez-Weinhouse MM, Shiota T, Imai M, Tsutsumi T, Sudo M, Endo N, Muroga Y, Hada T, et al. (2008) Potent antagonists of the CCR2b receptor. Part 3: SAR of the (R)-3-aminopyrrolidine series. *Bioorg Med Chem Lett* **18:**1869–1873.

Morphy R and Rankovic Z (2005) Designed multiple ligands. An emerging drug discovery paradigm. *J Med Chem* **48:**6523–6543.

Murphy PM (1994) The molecular biology of leukocyte chemoattractant receptors. *Annu Rev Immunol* **12:**593–633.

Palczewski K, Kumasaka T, Hori T, Behnke CA, Motoshima H, Fox BA, Le Trong I, Teller DC, Okada T, Stenkamp RE, et al. (2000) Crystal structure of rhodopsin: A G protein-coupled receptor. *Science* **289:**739–745.

Ribeiro S and Horuk R (2005) *Chemokine Receptor Antagonists: From the Bench to the Clinic.* Wiley-VCH, Weinheim, Germany.

Samson M, Labbe O, Mollereau C, Vassart G, and Parmentier M (1996) Molecular cloning and functional expression of a new human CC-chemokine receptor gene. *Biochemistry* **35:**3362–3367.

Schertler GFX (1998) Structure of rhodopsin. *Eye* **12:**504–510.

Seibert C, Ying W, Gavrilov S, Tsamis F, Kuhmann SE, Palani A, Tagat JR, Clader JW, McCombie SW, Baroudy BM, et al. (2006) Interaction of small molecule inhibitors of HIV-1 entry with CCR5. *Virology* **349:**41–54.

Stroke IL, Cole AG, Simhadri S, Brescia MR, Desai M, Zhang JJ, Merritt JR, Appell KC, Henderson I, and Webb ML (2006) Identification of CXCR3 receptor agonists in combinatorial small-molecule libraries. *Biochem Biophys Res Commun* **349:** 221–228.

Szekanecz Z, Szücs G, Szántó S, and Koch AE (2006) Chemokines in rheumatic diseases. *Curr Drug Targets* **7:**91–102.

Trabanino RJ, Hall SE, Vaidehi N, Floriano WB, Kam VW, and Goddard WA 3rd (2004) First Principles Prediction of the structure and Function of G protein-coupled receptors: validation for bovine rhodopsin. *Biophys J* **86:**1904–1921.

Vaidehi N, Schlyer S, Trabanino RJ, Floriano WB, Abrol R, Sharma S, Kochanny M, Koovakat S, Dunning L, Liang M, et al. (2006) Predictions of CCR1 chemokine receptor structure and BX 471 antagonist binding followed by experimental validation. *J Biol Chem* **281:**27613–27620.

Vriend G (1990) WHAT IF—a molecular modeling and drug design program. *J Mol Graph* **8:**52–56, 29.

Wise EL, Duchesnes C, da Fonseca PC, Allen RA, Williams TJ, and Pease JE (2007) Small molecule receptor agonists and antagonists of CCR3 provide insight into mechanisms of chemokine receptor activation. *J Biol Chem* **282:**27935–27943.

Zhang Y and Rollins BJ (1995) A dominant negative inhibitor indicates that monocyte chemoattractant protein 1 functions as a dimer. *Mol Cell Biol* **15:**4851–4855.

Address correspondence to: Nagarajan Vaidehi, Beckman Research Institute of the City of Hope, 1500 E. Duarte Road, Duarte, CA 91010. E-mail: nvaidehi@coh.org